Journal of Ceramic Processing Research. Vol. 14, No. 4, pp. 587~590 (2013)

J O U R N A L O F
Ceramic Processing Research

Improvement of crystal quality in semipolar GaN layer by using self-organized nanomasks on m-sapphire

Yongwoo Ryu, Joocheol Jeong, Jongjin Jang, Kyuseung Lee, Daehong Min, Jinwan Kim, Minho Kim, Seunghwan Moon, Geunho Yoo and Okhyun Nam*

LED Technology Center, Department of Nano-Optical Engineering, Korea Polytechnic University, Siheung 429-793, Korea

Semipolar GaN layers were grown on SiO_2 nanorods, which were fabricated by introducing self-organized masks to reduce defect density and to improve crystal quality. The decrease in the density of defects such as basal stacking faults, partial dislocations, and perfect dislocations was demonstrated by X-ray rocking curves for various planes. In addition, cross-sectional transmission electron microscopy images also confirmed the role of SiO_2 nanorods in blocking the defects. Further, the cathodoluminescence intensity of GaN layers grown on SiO_2 nanorods and the internal quantum efficiency of InGaN/GaN double quantum wells on SiO_2 nanorods were 9.5 times and 80% higher, respectively, than those of reference GaN layers. These higher values could be attributed to the improvement in the crystal quality of GaN layers due to the introduction of SiO_2 nanorods.

Key words: MOCVD, semipolar, nanorod, GaN.

Introduction

Many commercial GaN devices are grown on the c-plane. However, they are affected by spontaneous and piezoelectric polarization effects occurring in InGaN/GaN quantum wells (QWs) [1-2]. These polarization effects decrease device efficiency and luminescent output by separating electron and hole wave functions that increases radiative recombination lifetime [3-5]. Therefore, nonpolar and semipolar GaN have been studied by many research groups because of their structural properties that reduce the quantum-confined stark effect [6-7]. However, nonpolar and semipolar GaN grown on sapphire suffer from high defect density on the order of 10^{10} cm^{-2} for dislocations and 10^5 $cm^{-1}$for basal stacking faults (BSFs) [5, 8, 9]. Moreover, homo epitaxial growth, which is the best way of achieving high performance from nonpolar and semipolar GaN devices, is extremely difficult and expensive to realize through nonpolar and semipolar GaN substrates. To overcome these problems, various defect reduction techniques such as photo enhanced electrochemical etching to obtain nano porous GaN, use of patterned sapphire substrates, and epitaxial lateral overgrowth (ELO) have been introduced to improve the crystal quality of GaN [10-13]. Among these techniques, ELO is the best one. In this study, we propose a modified ELO technique based on the use of self-organized masks in semipolar GaN [13]. Semipolar GaN is used because of its various advantages such as thin coalescence thickness and low cost; moreover, the template quality of semipolar GaN can be easily improved.

*Corresponding author:
Tel : +82-31-8041-1916
Fax: +82-31-8041-1917
E-mail: ohnam@kpu.ac.kr

Experimental

A schematic for the fabrication of semipolar GaN nanorods is shown in Fig. 1. Firstly, a 2-μm-thick semipolar GaN layer was grown on m-plane sapphire by metal organic chemical vapor deposition (MOCVD). A 100-nm-thick SiO_2 layer was then deposited on this GaN layer by plasma-enhanced chemical vapor deposition, followed by the deposition of a Au film through evaporation by sputtering [Fig. 1(a)]. Three types of samples were prepared by controlling the Au-layer thickness in this process to obtain SiO_2 nanorods with diameters of 9, 12, and 15 nm [Figs. 2 (a)-(c)].

These multilayered samples were then subjected to rapid thermal annealing treatment under a N_2

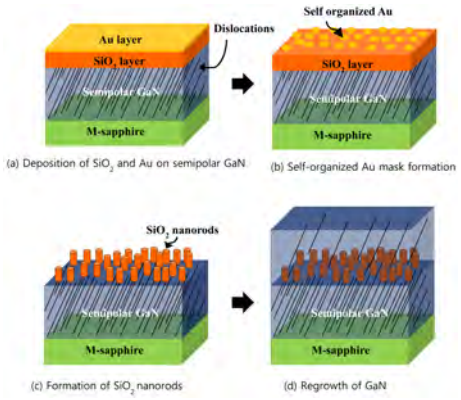

Fig. 1. The schematic diagram of fabricating semipolar nanorods embedded GaN.

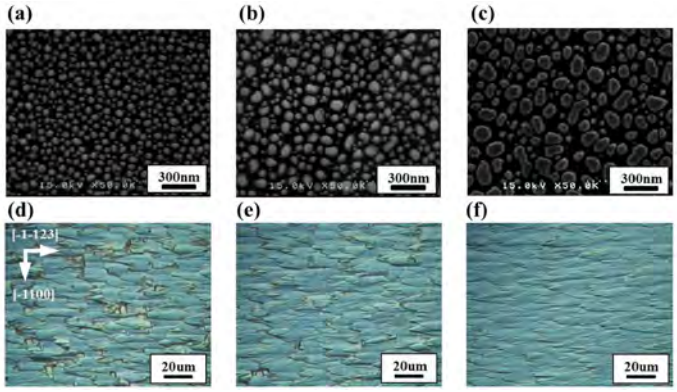

Fig. 2. SEM image of (a-c) the SiO_2 nanorods on semipolar GaN and OM images of (d-f) the semipolar GaN layers regrown on SiO_2 nanorods. The average diameters of SiO_2 are 50 nm ((a), (d)), 70 nm ((b), (e)) and 100 nm ((c), (f)], respectively.

atmosphere at 850 °C for 2 min to form self-organized Au nanoclusters [Fig. 1(b)].

The Au nanoclusters functioned as a mask in the etching of the underlying SiO_2 film and in the formation of SiO_2 nanorods on the GaN layer through the use of inductively coupled plasma.

Au nanoclusters were removed using aqua regia ($HCl : HNO_3 = 3 : 1$), andSiO_2nanorods finally remained on the semipolar GaN layer [Fig. 1(c)]. The semipolar GaN template with the nanorods was again subjected to MOCVD for overgrowth. Growth conditions such as pressure and flow rates of metal-organic sources were optimized to obtain good morphology for the GaN template with the nanorod layer. The total thickness of the semipolar GaN layer was approximately 5 μm [Fig. 1(d)]. Finally, InGaN/GaN double quantum wells (DQWs) were grown on reference and SiO_2-nanorod-inserted GaN layers. The DQWs consisted of 3.5-nm-thick InGaN wells and 12-nm-thick GaN barriers. The surface and cross-section morphologies of the semipolar GaN layers were observed by optical microscopy (OM) and scanning electron microscopy (SEM). High-resolution double-crystal X-ray rocking curves (DCXRCs) were measured for various planes of the semipolar GaN layers. The mechanism for the blocking of defects was observed by cross-section transmission electron microscopy (TEM). A cathodoluminescence (CL) analysis was performed to investigate the luminescence properties of the semipolar GaN layers. InGaN DQW structures were analyzed by temperature-dependent photoluminescence (TD-PL).

Results and Discussion

Fig. 2 (a)-(c) show the plan-view SEM images of SiO_2 nanorods on the semipolar GaN layers. The average diameters of the SiO_2 nanorods were 50, 70, and 100 nm. The coverage of the SiO_2 nanorods on the semipolar GaN layers was approximately 45% in all samples. Fig. 2 (d)-(f) show the OM images of semipolar GaN layers regrown on the SiO_2 nanorods. The surface morphologies of all the samples

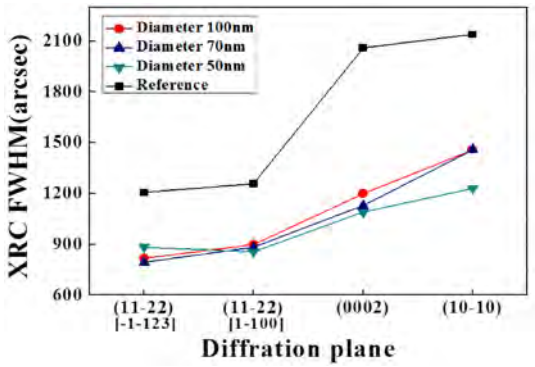

Fig. 3. The FWHMs of x-ray rocking curves of on- and off-axis planes of the SiO_2 nanorods inserted semipolar GaN layers as a function of diffraction planes.

Table 1. Diffraction planes associated with various defect types

Planes	$(11\bar{2}2)$		(0002)	$(10\bar{1}0)$
	$\Phi = 0°$	$\Phi = 90°$		
Defect type	PDs	PDs, PSFs	Perfect dislocation, PDs	BSFs

showedarrowhead-like features along the $[11\bar{2}3]$ direction; these features were triggered by anisotropic incorporation probability and the diffusion length of surface adatoms along crystallographic directions such as $[11\bar{2}3]$ and $[1\bar{1}00]$ due to crystallographic differencesbetween m-plane sapphire and semipolar $(11\bar{2}2)$ GaN. Moreover, it can be observed that the surface roughness reduced with an increase in the average diameter of the SiO_2 nanorods and in opening. This reduction can be attributed to easier nucleation upon larger opening.

Fig. 3 shows the full widths at half maximum (FWHMs) of the XRCs for the on- and off- axis diffraction planes. The FWHMs for the on-axis $(11\bar{2}2)$ XRC peaks along the $[11\bar{2}3]$ and $[1\bar{1}00]$ directions have been reported to be associated with partial dislocations (PDs) and/or prismatic stacking faults (PSFs), respectively (Table 1). The FWHMs for the $(11\bar{2}2)$ plane along the $[11\bar{2}3]$ and $[1\bar{1}00]$ directions for the reference sample were 1200 and 1260 arcsec,

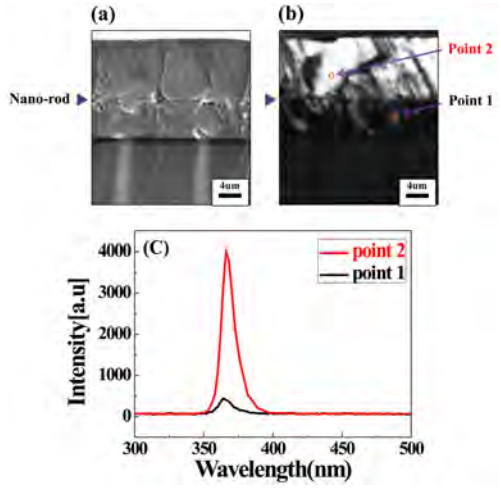

Fig. 4. The cross section (a) SEM image of the semipolar GaN grown on SiO_2 nanorods (Dia. = 100 nm), (b) a monochromatic CL image of the same region, and (c) CL spectra on the point 1 and point 2 in (b).

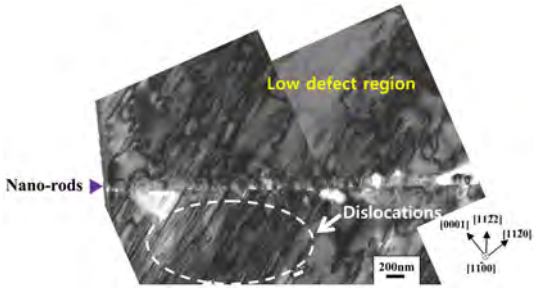

Fig. 5. The cross section TEM image of the semipolar GaN grown on SiO_2 nanorods (Dia. = 100 nm) viewed along [1$\bar{1}$00] using g = 0002.

respectively. The XRC FWHMs for all the SiO_2-nanorod-inserted GaN samples were approximately between 800 and 900 arcsec. It is known that the XRC FWHMs for the off-axis (0002) plane and the (10$\bar{1}$0) plane are related to PDs/perfect dislocations and BSFs, respectively, as listed in Table 1. The FWHMs for the (0002) and (10$\bar{1}$0) planes in the case of the reference sample were 2000 and 2150 arcsec, respectively. For all the SiO_2-nanorod-inserted GaN samples, the FWHMs for the (0002) plane varied between 1100 and 1200 arcsec, and those for the (10$\bar{1}$0) plane were 1130, 1460, or 1460 arcsec.

These results indicate that the introduction of SiO_2 nanorods could reduce a lot of defects such as PDs, perfect dislocations, PSFs, and BSFs. However, it should be noted here XRC measurements revealed that the extent of defect reduction did not depend on the diameter of the SiO_2 nanorods.

Cross-section SEM and CL images of the semipolar GaN layers grown on the SiO_2 nanorods (diameter = 100 nm) are shown in Figs. 4 (a) and (b). SiO_2 nanorod layers can be clearly seen in both the figures. The monochromatic CL image of the regrown GaN layer on the nanorods is brighter than that of the as-grown GaN layer on m-sapphire. Moreover, Fig. 4(c) shows that the CL

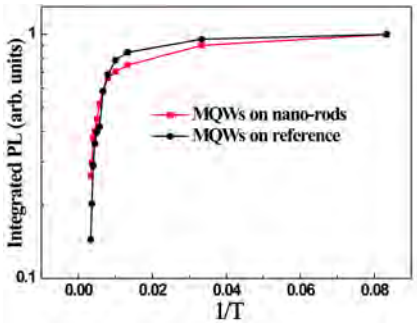

Fig. 6. Normalized integrated PL intensity as a function of temperature in an Arrhenius plots for the InGaN/GaN MQWs on reference and SiO_2 nanorods inserted GaN.

intensity at point 2 is 9.5 times that at point 1. These results indicate that the crystal quality of the overgrown GaN layer was significantly improved by the introduction of SiO_2 nanorods.

Fig. 5 shows a cross-sectional bright-field TEM image of the semipolar GaN layer grown on SiO_2 nanorods as viewed along the [1$\bar{1}$00] zone axis (g = 0002). It can be seen that the SiO_2 nanorods blocked defects such as PDs, which corresponds with the FWHMs of XRCs for the (0002) plane (Fig 3). Fig. 6 shows normalized integrated PL intensity data as a function of temperature in an Arrhenius plot for the InGaN/GaN DQWs on the reference and SiO_2-nanorod-inserted GaN layers for temperatures ranging from 13 to 300 K. The internal quantum efficiencies (IQEs) of InGaN/GaN QWs can be evaluated by integrating the PL intensity by assuming IQE to be 100% at low temperatures. Although the growth conditions were not fully optimized, the measured IQE of the DQWs was 26.3% for the SiO_2-nanorod-inserted GaN layer. This value is approximately 80% higher than that (14.4%) for the reference GaN layer. This finding reconfirms that SiO_2-nanorod inserted GaN layers can greatly improve the crystal quality of InGaN/GaN QWs.

Conclusions

We verified the effectiveness of SiO_2 nanorods in defect reduction and luminescence improvement for semipolar GaN. Semipolar GaN layers grown on SiO_2 nanorods had much lower defect density, a fact that was confirmed by XRC measurements. Moreover, cross-section TEM images showed that the SiO_2 nanorods functioned as blocking masks for the defects. In addition, the CL intensity of SiO_2-nanorod-inserted GaN layers was approximately 9.5 times that of reference GaN layers. Further, the IQE of the QWs on SiO_2 nanorods was approximately 26.3%, which was 80% higher than that of reference GaN layers. These observations confirmed the improvement in the crystal quality of semipolar GaN layers by the introduction of SiO_2 nanorods.

Acknowledgment

This work was supported by Industrial Strategic Technology Development Program No. 10041188 of the Ministry of Knowledge Economy and the National Research Foundation of Korea (NRF) grant funded by the South Korean government (MEST) No.2012R1A2A2A01011702.

Reference

1. T. Takeuchi, S. Sota, M. Katsuragawa, M. Komori, H. Takeuchi, H. Amano, and I. Akasaki, Jpn. J. Appl. Phys. 36 (1997) 382.
2. D.A. B. Miller, D.C. Chemla, T.C. Damen, A.C. Grossard, W. Wiegmann, T.H. Wood, and C.A. Burrus, Phys. Rev. B. 32 (1985) 1043.
3. J. S. Im, H. Kollmer, J. Off, A. Sohmer, F. Scholz, and A. Hangleiter, Phys. Rev. B. 57 (1998) 94-35.
4. L. Lahourcade, E. Bellet-Amalric, E. Monroy, M. Abouzaid, and P. Ruterana, Appl. Phys. Lett. 90 (2007) 131-909.
5. T.J. Baker, B.A. Haskell, F. Wu, J.S. Speck, and S. Nakamura, Jpn. J. Appl. Phys. Part. 245 (2006) 154.
6. S.M. Jung, S.-N. Lee, K. S. Ahn, and H.S. Kim, Electronic. Mater. Lett. 8 (2012) 1.
7. Y.S. Lee, T.H. Seo, A.H. Park, K.J. Lee, S.J. Chung, and E.K. Suh, Electronic. Mater. Lett. 8 (2012) 3.
8. T.J. Baker, B.A. Haskell, F. Wu, J.S. Speck, and S. Nakamura, Jpn. J. Appl. Phys. Part. 245 (2006) 154.
9. T. Gühne, Z. Bougrioua, P. Vennéguès M. Leroux, and M. Albrecht, J. Appl. Phys. 101 (2007) 113-101.
10. J.G. Jang, K.H. Lee, J.H. Hwang, J.C. Jung, S.A. Lee, K.H. Lee, B.H. Kong, H.H. Cho, O.H. Nam, J. Cryst. Growth. 361 (2008) 166-170.
11. M. Martyniuk, G. Parish, H. Marchand, P.T. Fini, S.P DenBaars, and L. Faraone, Electronic. Mater. Lett. 8 (2012) 2.
12. D.H. Lee, J.J. Jang, B.H. Kong, H.-K. Cho, and O.H. Nam, Jpn. J. Appl. Phys. 49 (2010) 058-001.
13. K. Xing, Y. Gong, J. Bai, and T. Wang, Appl. Phys. Lett. 99 (2011) 181-907.